Free Radical Catalysis by Galactose Oxidase

James W. Whittaker*

Department of Environmental and Biomolecular Systems, OGI School of Science and Engineering, Oregon Health and Science University, 20000 Northwest Walker Road, Beaverton, Oregon 97006

Received August 2, 2002

Contents

I. Introduction

The copper metalloenzyme, galactose oxidase [E.C. 1.1.3.9] (GO),[1−3] is an efficient oxidation−reduction catalyst utilizing an unusual free radical-coupled copper catalytic motif[1,4,5] in its active site for alcohol oxidation chemistry. This site combines two distinct one-electron acceptors, a Cu(II) metal center and a stable protein free radical, into a metalloradical complex that functions as a two-electron redox unit during catalytic turnover. The overall catalytic reaction is comprised of two separable half-reactions, oxidation of a primary alcohol and reduction of dioxygen to hydrogen peroxide:[6,7]

$$RCH_2OH \rightarrow RCHO + 2e^- + 2H^+$$

(substrate oxidation; oxidative half-reaction) (1)

$$O_2 + 2e^- + 2H^+ \rightarrow H_2O_2$$

(dioxygen reduction; reductive half-reaction) (2)

The recognition that free radical processes underlie all of the chemistry of galactose oxidase, from active site biogenesis and activation to catalytic turnover reactions, is contributing insight into the essential biochemical roles of free radicals. Interest in free radical catalysis[8−13] has been growing rapidly in recent years, driving the expanding field of free radical enzymology.[14,15]

Galactose oxidase is the best-characterized member of a family of enzymes known as radical-copper oxidases that includes another fungal enzyme, glyoxal oxidase,[16−20] the physiological partner of lignin peroxidase, and manganese peroxidase. The radical copper oxidase family has a broad phylogenetic distribution, and a prokaryotic homologue of galactose oxidase, the product of the *Stigmatella aurantiaca* fbfB gene, has recently been identified on the basis of nucleotide sequence analysis,[21] although the protein product of this gene, which appears to be involved in the developmental biology of the myxobacteria,[22] has not yet been characterized. Earlier structural[23] and spectroscopic work[1,4] on galactose oxidase, as well as current synthetic research aimed at synthetic modeling of active site structure and function,[24,25] has been thoroughly reviewed recently and will not be covered here. Theoretical approaches to understanding the chemistry of free radical enzymes is covered in a separate contribution in this issue.[26] This review will instead focus on research aimed at understanding the nature of the free radical site, the reactivity of the unique metalloradical complex, and the mechanism of free radical catalysis by galactose oxidase. A recent review of galactose oxidase in the context of bioinorganic enzymology concluded that "the time is now 'ripe' for an in-depth examination of the properties of the C−H bond cleavage step as well as the details of interaction with dioxygen",[27] and the present work may serve to measure progress toward understanding the mechanism of this interesting enzyme.

* Corresponding author. Telephone: 503-748-1065. Fax: 503-748-1464. Email: jim@ebs.ogi.edu.

10.1021/cr020425z CCC: $44.00
Published on Web 04/05/2003

James W. Whittaker received a B.Sc. in Biological Sciences from Sir George Williams University (now Concordia University) in Montreal and a Ph.D. in Biochemistry from the University of Minnesota (Minneapolis). He was an NIH postdoctoral fellow in Chemistry at Stanford University and subsequently joined the faculty of the Department of Chemistry of Carnegie Mellon University in Pittsburgh. In 1996, he moved to the Oregon Graduate Institute in Portland and is currently an Associate Professor in the Department of Environmental and Biomolecular Systems in the OGI School of Science & Engineering at Oregon Health & Science University. His research interests include free radical biochemistry and manganese metalloenzymes.

II. Protein Structure

Galactose oxidase is a 68 kDa monomeric fungal copper metalloenzyme enzyme secreted by *Fusarium spp.* into the extracellular environment, where it functions as a broad-spectrum catalyst for alcohol oxidation and a source of hydrogen peroxide.[4] The X-ray crystal structure of galactose oxidase[28−30] (Figure 1) shows that the folded polypeptide comprises three distinct domains. The N-terminal 155 residues form a globular domain containing a structural divalent metal binding site and a noncatalytic carbohydrate binding site that may function in targeting the enzyme. The catalytic domain (residues 155−552) comprises a 7-fold β propeller based on the *kelch* structural motif.[32] This β-propeller modular organization is common to a wide variety of eukaryotic ligand binding proteins, as well as a number of enzymes more closely related to galactose oxidase, including neuraminidase[33] (six-bladed propeller), methylamine dehydrogenase[34] (seven-bladed propeller), and methanol dehydrogenase[35] and nitrite reductase[36] (eight-bladed propellers). In galactose oxidase, this fold has been adapted to binding a single copper metal ion on the axis of the propeller domain to form a catalytic active site. The C-terminal domain (residues 553−639) caps the propeller on one face and donates a looping strand that threads through the axis of the propeller domain and contributes one of the metal ligands (His581) to the metal binding site.

The active site involves residues arising from remote regions of the polypeptide chain, brought together in the folded protein. Four amino acid side chains (from Tyr272, Tyr495, His496, and His581) directly coordinate a mononuclear Cu center in the protein, which is also bound by a solvent molecule to form a distorted five-coordinate metal complex (Figure 2). The bis-tyrosinate coordination of the copper ion in GO is unique among metalloenzymes. The organization of the metal complex places one of

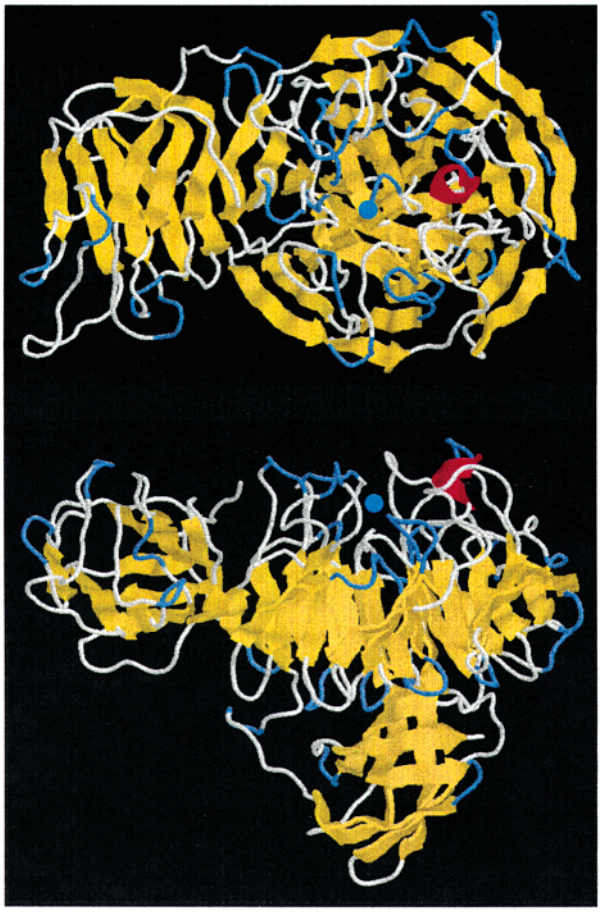

Figure 1. X-ray crystal structure of galactose oxidase. Two orthogonal views are shown, parallel (top), and perpendicular (bottom) to the axis of the β-propeller. Elements of protein secondary structure are color-coded (yellow, β sheet; magenta, α helix). The copper binding site is indicated by the cyan sphere. Based on PDB ID 1GOG and rendered with Rasmol (ref 31).

the tyrosines (Tyr272) roughly in the plane of the other ligands, leaving the second tyrosine (Tyr495) in the axial position of a fairly regular square-based pyramid. Alternatively, the coordination polyhedron may be viewed as a highly distorted trigonal bipyramid with the relatively long Cu-solvent vector defining the axial direction, and distortions between these limiting structures are involved in exogenous ligand interactions.[1,5] The orientation of the tyrosine rings within this complex is an important geometric factor determining the electronic interactions between the aromatic systems and the metal ion.[38] Ring torsion angles for both tyrosine ligands (Y272, Y495) in the galactose oxidase active site tend toward the perpendicular orientation that maximizes orbital overlap between the Cu valence shell and the O $2p_z$ orbital that is a part of the delocalized aromatic π-system of the ligand. These overlaps are predicted to be particularly critical for electronic coupling between the free radical Tyr272 phenoxyl ligand and the Cu(II) metal center.

The environment of the metal ion supports oxidation−reduction role by changing coordination number on reduction. X-ray absorption spectroscopy (XANES and EXAFS) probing the Cu(I)-containing GO supports a three-coordinate site for the reduced metal

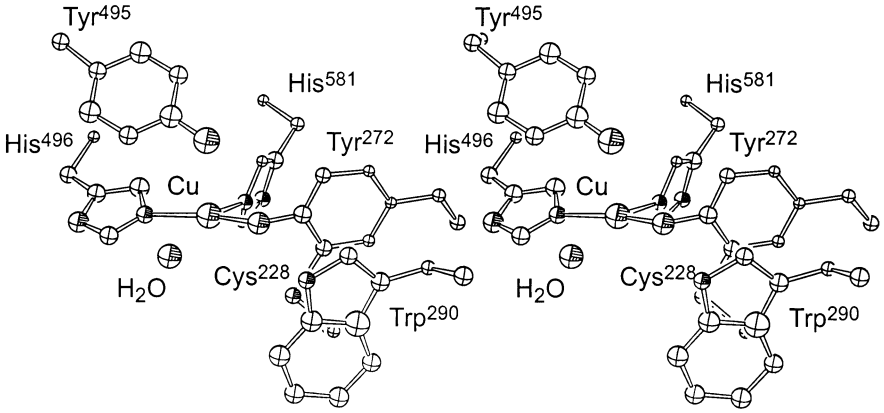

Figure 2. Stereoview of active site of galactose oxidase. Heteroatoms (O,N,S,Cu) are indicated by a shaded quadrant. Based on PDB ID 1GOG and rendered using ortep-3 (ref 37).

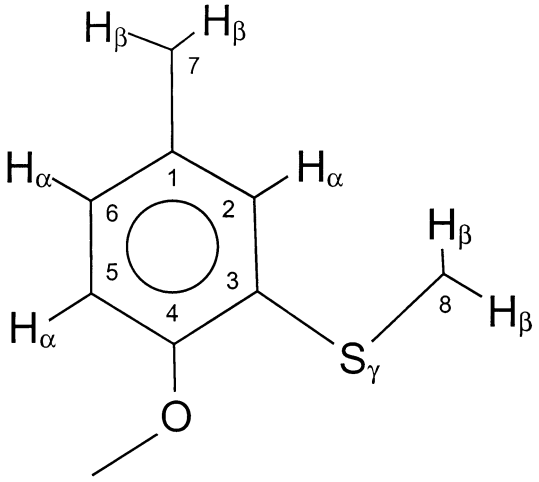

Figure 3. Structure of the tyrosine−cysteine cross-link site.

center,[39,40] consistent with retention of the trigonal planar set of Tyr272, His496, and His 581 in the complex and dissociation of Tyr495 and solvent. This type of low-coordinate ligand set is expected to be favorable for stabilizing a Cu(I) site in the protein during substrate oxidation. Further evidence for catalytic roles for specific residues in the active site complex is summarized below.

The most striking feature of this complex is the presence of a novel modified amino acid residue resulting from a covalent linkage between the S_γ of Cys228 and the C3 ring carbon of the Tyr272 aromatic side chain,[41] forming a Tyr−Cys cross-link (Figure 3). This cross-linked structure arises during protein biosynthesis through posttranslational covalent modification of the tyrosine side chain in a self-processing reaction that appears to occur spontaneously in the presence of copper and dioxygen without involvement of any other protein component.[42] The covalent cross-link is an essential feature of the active site structure. The Tyr−Cys cross-link has been shown to be redox-active and has been identified as the protein free radical site in galactose oxidase[43−45] (see below), where it functions as a redox cofactor. Although there is ample precedence for thiolate and thioether coordination to copper centers in proteins, there is no evidence for direct sulfur coordination to the metal ion in either oxidized or reduced form of galactose oxidase on the basis of either X-ray crystallography or EXAFS spectroscopy. The C228G variant is virtually inactive[46,47] (Table 1), leaving an extremely low residual level of activity that is in the range of missense translation errors in protein biosynthesis, making further quantitative interpretation somewhat equivocal.[48]

Table 1. Catalytic Proficiency of Galactose Oxidase Variants

mutational variant	relative catalytic activity	ref
WT	1.0	7
C228G	0.0001[a]	46
W290H	0.0005	46
Y495F	0.001	51
Y272F	n.d.	46

[a] For preparation containing 0.26 g-atom/mol Cu.

Tyrosine-495, the axial tyrosinate ligand in the copper complex, may function as a general base during catalysis. This role has been proposed on the basis of spectroscopic evidence for displacement of the axial tyrosine in anion complexes associated with uptake of a single proton.[49] This role is supported by structural studies, which show that the Cu−OTyr495 bond distance increases slightly (from 2.59 to 2.69 Å) when acetate replaces water in the complex. Conservative mutagenesis of Tyr495 to phenylalanine (Y495F) results in a 1100-fold decrease in catalytic activity and loss of proton uptake associated with anion binding.[50−52] Further evidence for a role of Tyr495 as a general base is provided by the temperature dependence of the structure of the Cu(II) complex of WT enzyme, reflected in the ligand field ($d \rightarrow d$) spectra of the metal ion. The transition has been interpreted as a conversion of an aquo complex with Tyr495 bound to a hydroxide complex with Tyr495 displaced, mimicking the changes that occur on anion binding and defining a putative proton-transfer coordinate in the active site involving Tyr495 and a *cis*-coordinated hydroxylic species[53] (Figure 4).

In addition to the four metal ligands and the cysteine component of the Tyr−Cys cofactor, a tryptophan residue (Trp290) has attracted special attention because of its close proximity to the Tyr−Cys cross-link. The tryptophan side chain lies parallel to the plane of the Tyr−Cys cofactor, the thioether side chain centered below the indole ring. The tryptophan

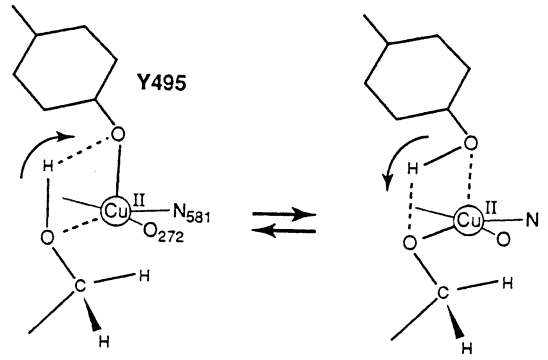

Figure 4. Proton-transfer coordinate in the galactose oxidase active site. Proton abstraction from hydroxylic ligands by Tyr495 results in displacement of tyrosine from the metal complex. The arrows indicate the direction of transfer of the proton across the hydrogen bond. The weakest interactions are indicated by broken lines. (From ref 53, reprinted with permission from Elsevier Science.)

side chain is oriented such that the indole N−H group is approximately aligned with the Tyr272 phenolic C−O vector. The role of Trp290 in the structure and function of the active site has been investigated by mutagenesis, replacing the indole ring with the imidazole side chain of histidine (W290H).[54] The W290H variant has been characterized both structurally (by X-ray crystallography) and functionally.[54] The stability of the active enzyme is reported to be significantly lower in the W290H mutant, supporting a role for the active site tryptophan in shielding the Tyr−Cys cofactor from exposure to solvent. The stacking of W290 with the Tyr−Cys cofactor is reminiscent of a related motif found in the quinoprotein methanol dehydrogenase, where a tryptophan residue lies parallel to the PQQ quinocofactor.[35]

III. The Free Radical Site

The unusual two-electron reactivity of the mononuclear copper active site in galactose oxidase has been explained in terms of the direct participation of the protein in the redox chemistry of the active site, forming a stable free radical−copper complex in the active enzyme.[7] The copper-free apoprotein is readily oxidized under mild conditions, forming a stable free radical, with distinctive optical absorption and electron paramagnetic resonance (EPR) spectra[43] (Figure 5). A single free radical species is observed, implying a unique reactive site in the protein. At X-band (9 GHz) the EPR spectrum exhibits an average g-value of 2.005 and a complex pattern of fine structure splittings. Isotopic labeling demonstrates that the free radical site in the apoprotein is derived from a tyrosine residue, and it allows the major splittings to be assigned to hyperfine interactions between the unpaired electron and the β hydrogens in the side chain of a perturbed tyrosine residue.[43] ENDOR spectroscopy (also at X-band) yields more refined estimates of the hyperfine coupling constants and provides evidence for hydrogen bonding to the phenoxyl oxygen[44] (Table 2).

High-frequency EPR spectroscopy has proven to be a particularly effective tool in the characterization

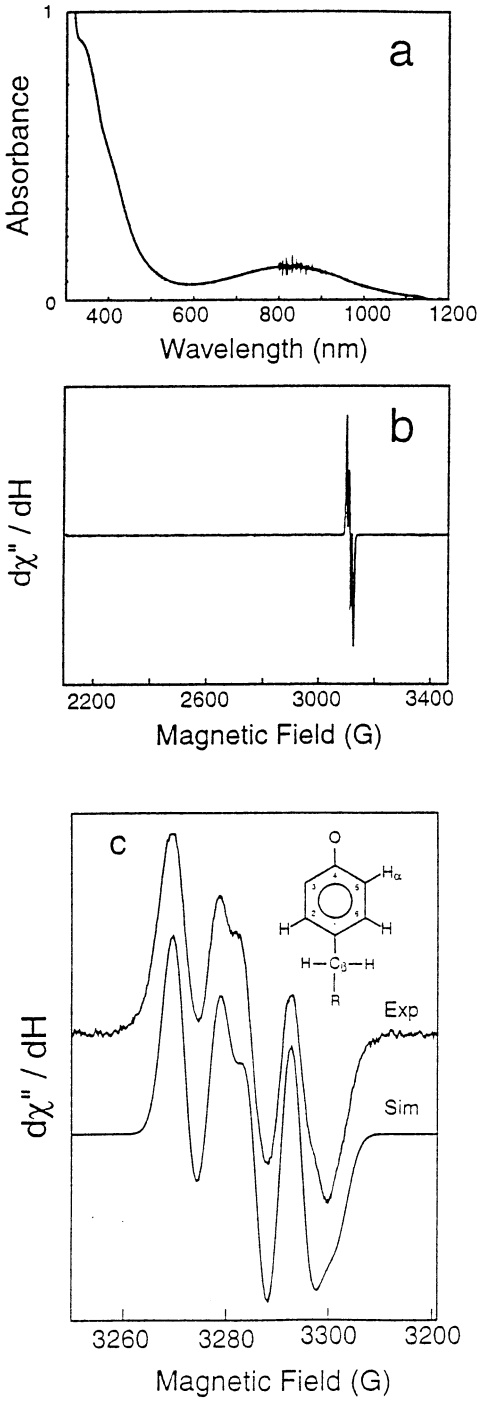

Figure 5. Free radical spectra for apo-galactose oxidase. (a) Optical absorption spectrum for free radical containing apogalactose oxidase (15 mg/mL, following treatment with hexacyanoferrate(III)). (b) EPR spectrum for apogalactose oxidase free radical. Instrumental parameters: microwave power, 0.03 microwatts; microwave frequency, 9.220 GHz; modulation amplitude, 5 G; temperature, 8 K. (c) Expansion of X-band EPR spectrum for apogalactose oxidase free radical. (From ref 1.)

of this (and other) biological free radicals,[55] since at high magnetic field the intrinsic electronic **g**-anisotropy dominates over the electron−nuclear hyperfine interactions, allowing a more detailed analysis of the spectrum. The high frequency (139.5 GHz) EPR spectrum for the apogalactose oxidase free radical[45] shown in Figure 6 illustrates the dramatic simplification that is achieved by this approach. The spec-

Table 2. Spectroscopic Characterization of Apogalactose Oxidase and Model Free Radicals

free radical	ν (GHz)	T (K)	spectroscopic parameters		ref
			ApoGO•		
EPR	9	77	$g_{av} = 2.005$	$A^{\beta} = 15$ G	43
	139.5	10	$g_x = 2.00741$	$A_x^{\beta}7 = 15.5$ G	45
			$g_y = 2.00641$	$A_y^{\beta}7 = 14.2$ G	
			$g_z = 2.00211$	$A_z^{\beta}7 = 14.2$ G	
				$A_x^{\beta}8 = 9.5$ G	
				$A_y^{\beta}8 = 8.0$ G	
				$A_z^{\beta}8 = 8.5$ G	
ENDOR	9	10		$A_{iso}^{\beta} = 14.6$ G	44
optical absorption		300	320 nm (9000)[a]		43
			400 nm (5500)		
			800 nm (1800)		
			mtc•[b]		
EPR	9	77	$g_{av} = 2.005$		56
	9	120	$g_x = 2.0095$	$A_{av}^{\beta} = 9.28$ G	57
			$g_x = 2.0067$		
			$g_x = 2.0023$		
	9	243	$g_{av} = 2.006$	$A^{\beta} = 8.6$ G	58
	139.5	10	$g_x = 2.0072$	$A_x^{\beta} = 9.2$ G	45
			$g_x = 2.0062$	$A_y^{\beta} = 9.2$ G	
			$g_x = 2.0019$	$A_z^{\beta} = 9.2$ G	
calcd			$g_x = 2.0060$		45
			$g_x = 2.0044$		
			$g_x = 2.0023$		
calcd[e]			$g_x = 2.0079$		61
			$g_x = 2.0052$		
			$g_x = 2.0025$		
optical absorption		77	400 nm[c]		56
			830 nm		
		77	350 nm[d]		57
			400 nm		
			850 nm		

[a] λ_{max} (extinction coefficient, $M^{-1}cm^{-1}$). [b] mtc•, 2-(methylthio)cresyl phenoxyl free radical. [c] Prepared by photooxidation in propionitrile:butyronitrile glass. [d] Prepared by pulse radiolysis in N_2O-saturated aqueous solution (pH 11). [e] Calculated for 2-thio phenoxyl free radical.

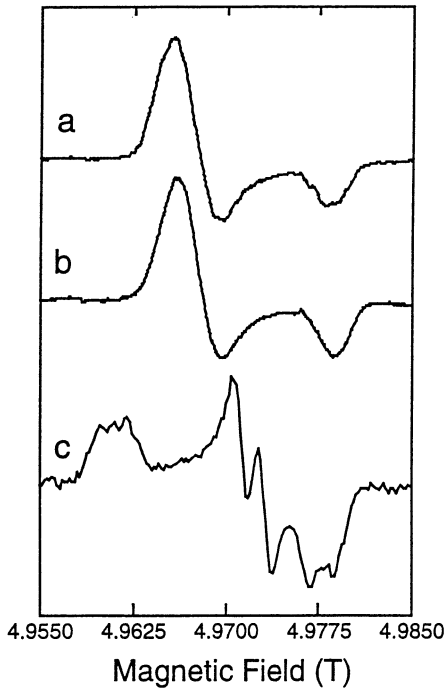

Figure 6. High-frequency (139.5 GHz) EPR spectra for biological free radicals. (a) Apogalactose oxidase free radical. (b) 2-(Methylthio)cresyl phenoxyl free radical. (c) Ribonucleotide reductase free radical. (From ref 1.)

trum displays an axial line shape ($g_x = g_y > g_z$) that is clearly distinct from the rhombic line shape ($g_x \neq g_y > g_z$) characteristic of a simple tyrosyl phenoxyl free radical like that found in ribonucleotide reductase. The axial spectrum of the apogalactose oxidase free radical is reproduced nearly exactly by the 2-(methylthio)cresyl free radical formed by photooxidation of a model for the Tyr−Cys site in the protein. Thioether substitution restricts the oxidation chemistry of the phenol to well-resolved single-electron steps, in contrast to hydroquinones which readily undergo two-electron oxidation. This constraint ensures that the Tyr−Cys cofactor in the protein serves as a free radical redox site. The optical absorption spectrum of the 2-(methylthio)cresyl free radical[56,57] (Figure 7) closely resembles the spectrum of the apogalactose oxidase radical, confirming that the free radical is localized on the Tyr−Cys side chain.

The spectroscopic analysis has been complemented by theoretical studies aimed at understanding the unique characteristics of the tyrosyl-cysteinyl free radical[45,57−62]. Calculations of the free radical ground-state electronic structure of the 2-(methythio)cresyl model radical agree that the spin occupied molecular orbital (SOMO, a" symmetry) is delocalized over the ring system, with a major contribution from the phenoxyl oxygen p_z orbital (Figure 8). The thioether sulfur also involved in the SOMO wave function, with normalized orbital contributions ranging from 0.12 to 0.28, depending on the method used for the calculation. Despite being fairly small values, the thioether sulfur contributions are expected to be

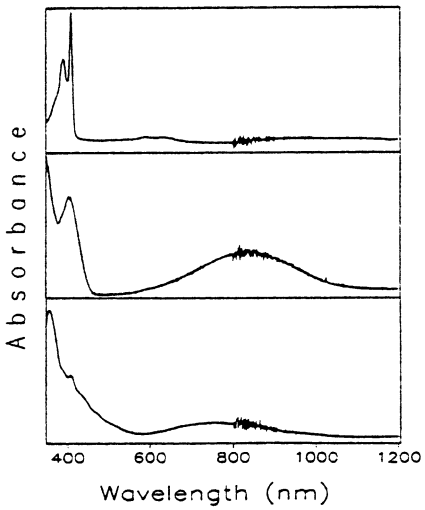

Figure 7. Low-temperature optical absorption spectra for model phenoxyl free radicals. (top) Cresyl phenoxyl free radical. (middle) 2-(Methylthio)cresyl phenoxyl free radical. (bottom) 2-(Methylsulfinyl)cresyl phenoxyl free radical. All samples prepared by UV photooxidation in propionitrile: butyronitrile glass; temperature, 77 K. (From ref 56.)

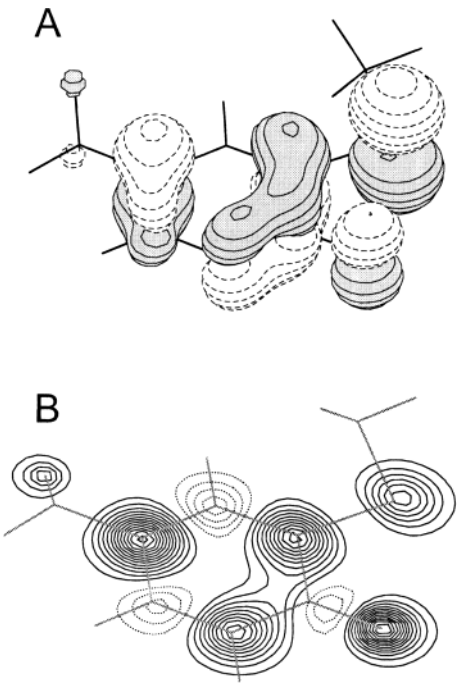

Figure 8. Electronic structure of the thioether-substituted phenoxyl free radical. (A) SOMO contoured at 0.05 e/au^3. (B) Total spin density for phenoxyl ground state, evaluated over surface raised 1.5 au above the plane of the ring carbon atoms. (α spin density, —; β spin density, ---). Rendered using molden (ref 63.)

important for the stabilization of the radical. The calculations support a picture of odd-alternant spin distribution in which the unpaired electron density is greatest on alternating atoms within the delocalized π-system, reflecting the nodal character of the SOMO electronic wave function.

The analysis of the ground-state electronic structure has been extended through calculations of the **g**-tensor for the protein and model radicals.[45,61] Interestingly, the calculations that predict a relatively small involvement of the thioether sulfur in

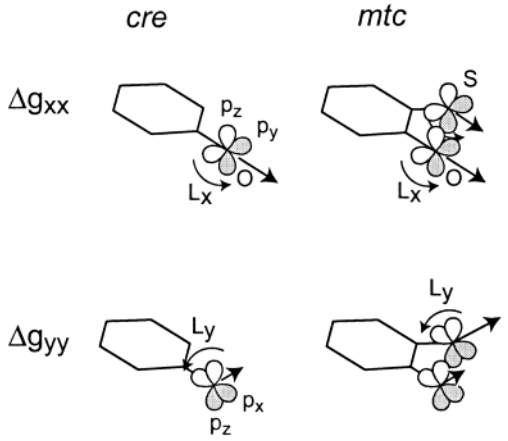

Figure 9. Model for orbital *g*-shifts for substituted phenoxyl free radicals. cre, cresyl phenoxyl free radical; mtc, 2-(methylthio)cresyl phenoxyl free radical. Components of the **g**-tensor (Δg_{xx}, Δg_{yy}) arise from spin−orbit mixing (via matrix elements of L_x, L_y) in a gauge invariant sum over all atomic contributions.

the SOMO lead to more rhombic **g**-tensor, while the calculations that indicate a more substantial contribution of the Tyr−Cys sulfur lead to more axial *g*-values, closer to the experimental results. A simple model has been proposed[45] to explain the distinctive axial spectrum observed for the apogalactose oxidase and 2-(methylthio)cresyl free radicals, on the basis of the origin of the g-shifts in atomic valence spin−orbit mixing effects. The molecular **g**-shift arises as a gauge-invariant sum over the individual atomic contributions that result from coupling between the electronic spin angular momentum localized on the atom and the orbital angular momentum of the valence orbital set. In the thioether substituted phenoxyl free radicals, the oxygen and sulfur atoms will contribute the largest spin−orbit effects. The largest orbital contributions for those two atoms (g_x, g_y) lie in the plane of the aromatic ring and are mutually orthogonal, as a result of the orientation of the nonbonding valence orbitals on the two atoms (Figure 9). As a consequence, the **g**-anisotropy that would result from either of the two contributions individually is approximately canceled out, and an approximately axial **g**-tensor is observed. This detailed characterization of the free radical site in apogalactose oxidase has provided important information on the nature of the thioether substituted phenoxyl free radical that is the protein redox site in the copper-containing holoenzyme.

The protein may be expected to perturb the structure of the free radical through hydrogen-bonding and ring-stacking interactions, altering the pattern of unpaired electron density and providing mechanisms for delocalization of the unpaired electron over a more extended region. As indicated above, the ENDOR studies on the apogalactose oxidase free radical provide evidence for hydrogen bonding between the phenoxyl oxygen and neighboring residues or solvent. On the other hand, high-frequency EPR measurements demonstrate that there is no significant delocalization of the unpaired electron spins into the π-system of the stacked tryptophan W290.

Scheme 1. Redox Interconversion of Galactose Oxidase Species

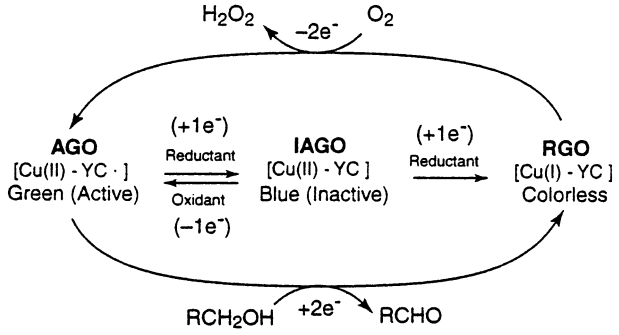

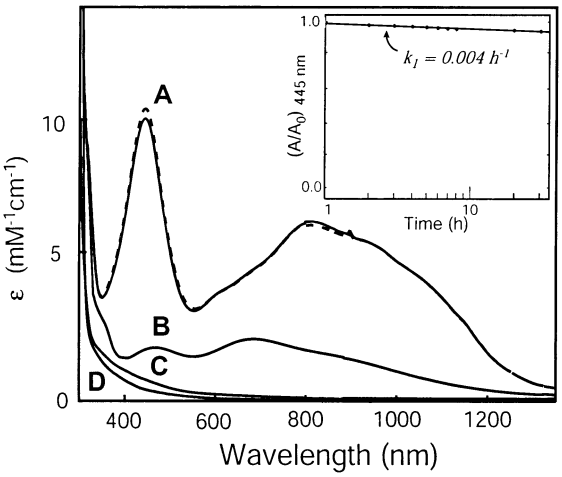

Figure 10. Optical absorption spectra for galactose oxidase in accessible redox states. (A) Redox-activated enzyme (AGO) (pH 5.6, ---; pH 7.3, —). (B) One-electron reduced inactive enzyme (IAGO). (C) Substrate-reduced anaerobic enzyme. (D) Metal-free apoprotein. The insert shows the kinetics of spontaneous decay of the active enzyme, with $t_{1/2}$ = 7.2 d. (From ref 71)

IV. The Radical Copper Complex

A. Spectroscopic Characterization

In contrast to the one-electron reactivity typical of a mononuclear copper complex converting between Cu(II) and Cu(I) oxidation states, galactose oxidase exhibits three distinct redox forms associated with two one-electron oxidation−reduction steps, each form being distinguished by a characteristic spectroscopic signature.[1,4,7,64] The fully oxidized (AGO) and fully reduced (RGO) forms are catalytically active, while the intermediate oxidation level is catalytically inactive (IAGO) (Scheme 1). The fully reduced form contains Cu(I) in a low-coordinate complex. EXAFS studies are consistent with three-coordination at copper in the reduced complex, suggesting that the trigonal planar set of ligands (Tyr272, His496, and His581) is retained, forming a favorable T-shaped arrangement of ligands.[40] The inactive form has been characterized as a simple Cu(II) complex on the basis of EPR and XANES.[7,39] Oxidation of this complex with mild oxidants (e.g., hexacyanoferrate (III)) results in conversion to active enzyme exhibiting an unusual intense optical spectrum (Figure 10). This active oxidized species contains Cu(II) and results from oxidation of the protein rather than the metal ion, forming a free radical-coupled copper active site.

Scheme 2. Ground State Interactions in the Free Radical-Coupled Copper Complex

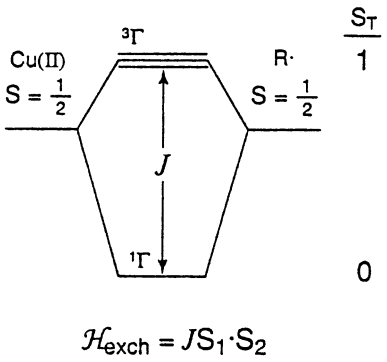

$$\mathcal{H}_{exch} = JS_1 \cdot S_2$$

Table 3. Reduction Potentials for Galactose Oxidase Species

	$E°'$[Cu(II)/Cu(I)] (mV)[a]	$E°'$[TyrCys•/TyrCys] (mV)[a]	ref
WT	+450[b]	7	
	+150[c]	+400[c]	67
	−300−500[d]	68	
C228G	+630	67	
W290H	+730	67	
Y495F	+169	+450	67
Apo	+570	67	

[a] Versus NHE. [b] Spectrophotometric titration. [c] Kinetic method. [d] Predicted on the basis of semiquantitative reaction energy profile.

Antiferromagnetic coupling of unpaired electron spins on the copper ion, and the free radical ligand leads to stabilization of an EPR-silent diamagnetic ground state (Scheme 2). A paramagnetic triplet state is found by multifield magnetic susceptibility[65] to lie at least 200 cm^{-1} higher in energy.[53] Resonance Raman spectroscopy of the radical copper complex shows that both modified and unmodified tyrosines contribute to the valence shell excitations, suggesting that the radical copper complex may be stabilized in the protein by delocalization of the radical character over both tyrosine ligands, a ligand-to-ligand charge transfer (LLCT) mechanism.[66]

B. Redox Chemistry

The redox potential for conversion of GO to the active form by oxidation of the Tyr−Cys cofactor has been determined by spectrochemical titration as +0.45 V (vs NHE),[7] significantly lower than that estimated for oxidation of the 2-(methylthio)cresol phenolic model compound.[56−59] Reduction potentials have been determined for WT and mutant GO variants for both the free radical site and the metal center (Table 3).[67] Elimination of the axial tyrosine interaction (Y495F) results in a modest increase of the Cu(I)/Cu(II) redox couple (+16 mV) but has a more substantial effect on the Tyr−Cys redox potential, which is raised by 50 mV in the mutant. This supports a role for Tyr495 in stabilizing the free radical complex through LLCT delocalization in the resting enzyme. The consequences of W290H GO mutagenesis are even more dramatic, raising the Tyr−Cys redox potential to 730 mV, a 330 mV shift to higher potential from the value obtained for the WT enzyme. The strong perturbation of W290H

mutagenesis implies that the interaction between the Tyr−Cys and tryptophan side chains has a significant stabilizing effect on the Tyr−Cys redox couple, even though there is no evidence for delocalization of the radical over the indole moiety. Solvent shielding may be a more important role for the tryptophan, restricting the hydrogen bonding character of the cofactor environment. The analysis of the C228G variant is more problematic, since the protein contained only about 26% of the full copper complement and the spectral changes that were induced by titration with a strong oxidant could not be assigned to a specific process.

The as-isolated enzyme typically is a mixture of oxidation states, with IAGO and AGO forms predominating (in a ratio ranging between 20:1 to 1:1 between preparations[1,7,69]). This variability in the oxidation state, and the instability of the redox-activated enzyme under normal handling and its sensitivity to commonly used buffers, has led to a proposal that the enzyme undergoes "autoredox interconversion" between IAGO and AGO forms in solution.[69] The autoredox process is proposed to determine the steady-state level of AGO through competition between reductive and oxidative reactions, and a disulfide group in the protein has been identified as an important relay point involving a disulfide radical anion intermediate.[69,70] However, the source of the extremely low-potential reducing equivalents required for disulfide radical anion formation driving the autoredox interconversion has never been established. In any case, the autoredox behavior appears to be inconsistent with the observation that the AGO enzyme is stable for weeks in the absence of exogenous reductants.[71] This stability allows the enzyme to be prepared in a homogeneous active form in order to characterize its catalytic properties. The discussion of the free radical mechanism of galactose oxidase catalysis will be introduced with a brief summary of the special features associated with free radical catalysis.

V. Principles of Free Radical Catalysis

Free radicals are molecules with unpaired electrons in their valence shell either as a consequence of having an odd number of electrons (leaving at least one unpaired, as in one-electron oxidized amino acid side chains in proteins) or an orbital degeneracy that leads to stable electron unpairing in the ground state (as occurs in dioxygen). These molecules are intrinsically different from the majority of chemical species in which electrons are fully paired, and the differences are clearly expressed in their chemical reactivity. The chemistry of free radicals is dominated by one-electron reactions, including single electron transfer (SET), hydrogen atom transfer (HAT), and proton-coupled electron transfer (PCET). These three elementary processes underlie the vast majority of free radical mechanisms in organic chemistry, and a comprehensive review of the field has recently appeared. Each process will be briefly summarized in this section, providing the framework for discussion of the catalytic mechanism of galactose oxidase.

A. Single Electron Transfer

Single electron-transfer involves simple one-electron oxidation of a redox partner, resulting in reduction of the radical. Conservation of electronic charge results in complementary changes in the net charges on each of the species involved, and conservation of angular momentum requires that SET involving a free radical reactant ($S > 0$) must lead to formation of at least one radical product:

$$X\bullet + YH \rightarrow X^- + YH\bullet^+ \qquad (3)$$

The reaction is written in terms of reduction of the free radical, although for quinonoid species, oxidation would also be possible. The hydrogen in eq 3 is included to emphasize that the oxidized and reduced species often exhibit dramatically perturbed pK_a values for hydrogens associated with heteroatoms in the structures. The electrostatic consequences of electron transfer are reflected in acidity, with X^- being more basic and $YH\bullet^+$ more acidic than their precursors, leading to a pH dependence of SET rates. The rate of SET is governed by both the driving force and geometric factors involving orbital overlaps, which have been extensively discussed in the more general terms of long-range SET.[72,73] The quantum mechanical character of the electron is reflected in the geometric (orbital) dependence of the SET process, involving overlap of the donor and acceptor orbital wave functions.

The change in electronic occupation of molecular orbitals has important consequences for chemical reactivity. Removing electrons from bonding orbitals (or, conversely, adding electrons to antibonding orbitals) will result in molecular destabilization that may contribute significantly to catalytic activation. To the extent that the orbital is localized, singly occupied MO can be described as a one-electron bond, which is weaker than the typical two-electron bond in which much of chemistry is framed. Free radicals thus make molecules more susceptible to bond cleavage processes.

B. Hydrogen Atom Transfer

The most common bond cleavage process associated with free radical reactions is hydrogen atom transfer (HAT)[74−79] in which the elements of hydrogen (a proton and an electron) are simultaneously abstracted from the substrate. This reaction is favorable for several reasons. Hydrogen is univalent, and its bonding patterns lead to exposure on the molecular periphery. Hydrogen abstraction involves breaking a single bond. Concerted transfer of a proton and electron provides charge compensation that avoids unfavorable charge separation in the reaction

$$X\bullet + YH \rightarrow XH + Y\bullet \qquad (4)$$

The hydrogen atom is sufficiently light to exhibit quantum mechanical effects, e.g., tunneling through a barrier, as a consequence of its relatively long de Broglie wavelength. The amplitude of the nuclear coordinate wave function that permits transmission of a particle through a potential barrier decays

Scheme 3. Alternative Pathways for Proton-Coupled Electron Transfer

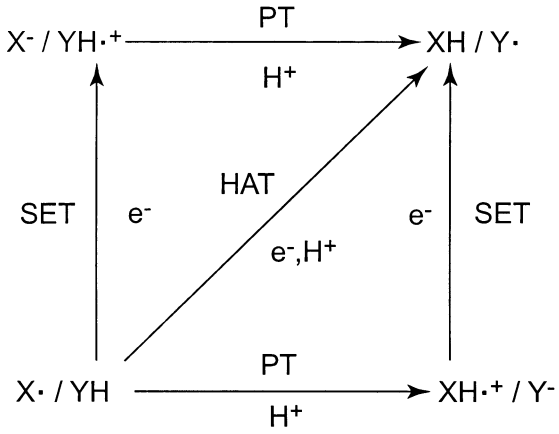

rapidly away from the equilibrium position, resulting in a strong orientation and distance dependence for hydrogen atom tunneling. The experimental signature of tunneling kinetics is anomalous isotope effects and temperature dependence. The driving force for HAT is based on the relative stability of the hydrogen in the initial and final states of the reaction, which in simplest terms can be analyzed in terms of X−H and Y−H bond enthalpies.[79] The bond dissociation energy for the phenolic O−H group is 86.2 kcal/mol,[80] strong enough to support hydrogen atom abstraction and to contribute to the surprisingly high reactivity of phenoxyl radicals.[81] Bond strength is an important determinant of reactivity and determines the strength of coupling between proton and electron transfer. In recent years theoretical and experimental studies have explored the spectrum of reactions, and it is now clear that there is a continuous spectrum of processes involving proton-coupled electron transfer.

C. Proton-Coupled Electron Transfer

Proton coupled electron transfer (PCET) is the most general process, associated with nonconcerted or stepwise reaction. The nonconcerted transfer of a proton and an electron implies either spatial or temporal resolution of the two elementary processes, and the two components (H^+,e^-) may take distinct paths between donor and acceptor forming discrete reaction intermediates (Scheme 3). Alternatively, the electron and proton donor/acceptor pairs may be distinct species, the coupling defined by the energetics of the interacting groups. Hydrogen atom transfer thus represents a limiting case of PCET in which both proton and electron motions are concerted and synchronous. More generally, PCET can occur in discrete, sequential steps with either proton or electron-transfer events occurring first, although all degrees of dynamical correlation are in principle possible.[82,83]

VI. Experimental Approaches to the Catalytic Mechanism

The galactose oxidase turnover reaction may be functionally decomposed into two separate and distinct half-reactions (substrate oxidation, O_2 reduction).[7] These half-reactions are resolved in practice by eliminating one or other of the reactants (substrate, O_2), allowing the enzyme to be reduced by its hydroxylic substrate anaerobically and subsequently reoxidized by O_2. This behavior is consistent with ping-pong reactivity:[7,71,84,85]

$$E_{ox} + S \xrightarrow{k_{red}} E_{red} + P \quad (5)$$

$$E_{red} + O_2 \xrightarrow{k_{ox}} E_{ox} + H_2O_2 \quad (6)$$

Kinetic analyses can be performed either through measuring the biomolecular reaction with one substrate to characterize a single half-reaction, or by monitoring turnover. Both approaches have proven useful in studies of galactose oxidase catalysis.

A variety of steady-state methods have been developed for measuring galactose oxidase turnover. Many of these take advantage of well-developed techniques for measuring oxygen and its reduction product, hydrogen peroxide. Polarographic methods for determining O_2 concentration (e.g., the Clark oxygen electrode) provide a convenient approach for monitoring the oxygen uptake in the oxidizing half-reaction (eq 7) using a variety of reducing substrates.[86] These assays are typically performed in the presence of an oxidant (ferricyanide) which ensures that the full activity is expressed.[86] Galactose oxidase turnover may also be coupled to a peroxidase-linked chromogenic reaction providing high sensitivity detection of galactose oxidase activity.[87] In the coupled reaction, the peroxidase enzyme is able to activate galactose oxidase, eliminating the need for additional oxidants. A direct assay has also been developed on the basis of the absorption of the conjugated carbonyl product from benzyl alcohol (alternative substrate) oxidation.[87] The direct assay method has been used to distinguish between catalytically active and inactive forms of the as-isolated enzyme.[7]

A. Rapid Kinetic Studies

Both oxidation and reduction half-reactions are extremely fast and push the limits of stopped flow kinetic analysis. Studies of the alcohol oxidation half-reaction are additionally challenging because of the requirement for strict anaerobiosis (to avoid turnover processes) combined with the restriction that reductants (such as dithionite) typically used to establish anaerobic conditions must also be excluded, to maintain the oxidized state of the active enzyme. This problem has been successfully solved by using a efficient oxygenase-based scrubbing system to remove oxygen from the stopped flow instrument.[88] Using these approaches it has been possible to measure the direct reduction of active GO by its reducing substrate at reduced temperature (4 °C).[71] The kinetic parameters for this reaction are similar to those obtained by monitoring the reaction in the steady state. The bimolecular reaction is saturable with a K_d of 180 ± 20 mM for formation of the initial complex, similar to the Michaelis constant obtained by monitoring the steady-state reaction (175 mM at saturating concentrations of O_2).[84]

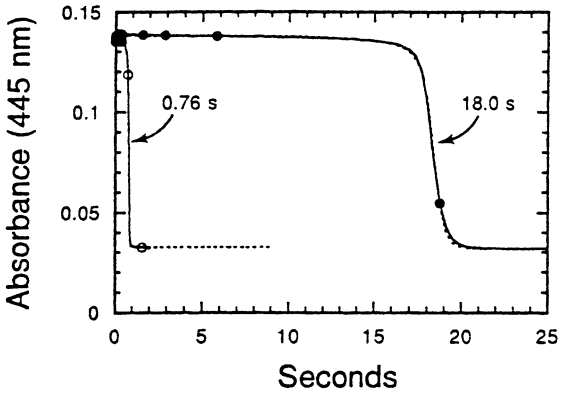

Figure 11. Enzyme monitored turnover reactions. Galactose oxidase (approximately 11 μM final concentration) was mixed with 5 mM reducing substrate (either 1-*O*-methyl-6,6′-di-[^{1}H]-α-D-galactopyranoside, ○, or 1-*O*-methyl-6,6′-di-[^{2}H]-α-D-galactopyranoside, ●) in air-saturated buffer (50 mM sodium phosphate) at 4 °C. The experimental curves were fit to the differential equations for ping pong turnover reaction using the kinetic parameters in Table 4. (From ref 71.)

Table 4. Kinetic Parameters for Galactose Oxidase Turnover[a]

substrate	k_{red} ($\times 10^4$ M^{-1} s^{-1})	k_{ox} ($\times 10^6$ M^{-1} s^{-1})	ref
1-*O*-methyl-α-D-galactopyranoside	1.53	7.99	71
D-galactose	0.93	0.98	90
2-deoxy-D-galactose	0.8	1.03	90
1-*O*-methyl-*β*-D-galactopyranoside	1.2	1.0	90
D-raffinose	1.72	1.01	90
dihydroxyacetone	2.74	1.02	90

[a] In buffered solution, pH 7.

An alternative method for kinetic characterization of the turnover reaction is based on the enzyme-monitored turnover method,[89] taking advantage of the chromophoric character of the enzyme to monitor its state during turnover. The relatively fast reaction of GO with O_2 ensures that the enzyme is essentially all in the oxidized state during turnover until virtually all the dioxygen is consumed, at which point the excess of reducing substrate rapidly converts the enzyme to the colorless reduced form. This second phase provides a direct measure of the kinetics of reoxidation by dioxygen. Since the overall reaction is rate-limited by substrate reduction, the duration of the first phase reflects the time required to perform the discrete number of catalytic turnovers and provided information on the substrate oxidation kinetics. Typical kinetic traces[71] are shown in Figure 11. One advantage of this approach is that it permits kinetic characterization of both reductive and oxidative half-reactions from a single timecourse and is relatively independent of hydrodynamic mixing constraints of the stopped flow system.

Kinetic parameters extracted from enzyme monitored turnover measurements (Table 4) are very similar to those obtained by measuring direct reduction in the isolated half-reaction and by oxygen uptake steady-state kinetics. This supports the bimolecular character of substrate interactions well below the K_m and an essentially collisional reaction with substrate under physiological conditions. The enzyme monitored turnover studies have been extended[90] to include a range of reducing substrates (Table 4), and the interesting result emerges that the reoxidation kinetics are virtually independent of the nature of the reducing substrate, even when the reduction rates varied 5-fold. Slightly different values for the individual kinetic constants obtained in these independent studies by two groups have been attributed to differences in estimating the concentration of active enzyme in the reactions.[71]

B. Isotope Kinetics

Isotope effects on enzyme kinetics can provide important insight into reaction mechanisms. Isotope studies in early work on galactose oxidase established the *pro*-S stereospecificity of hydrogen abstraction from the substrate alcohol[91] and provided an estimate of the deuterium kinetic isotope effect of methylene-deuterated substrate under steady-state turnover conditions (k_H/k_D = 7.7 for 1-*O*-methyl-6,6′-di-[^{2}H]-*β*-D-galactopyranoside using peroxidase coupled assay,[91] and k_H/k_D = 8.7 for 1-O-methyl-6,6′-di-[^{2}H]-α-D-galactopyranoside from V/K_m measurements monitored by oxygen uptake[92]). Simple halo alcohols give smaller KIEs in the range 3.1−3.9[93] and measurement of KIE for a homologous series of substituted benzyl alcohol derivatives shows a significant substituent dependence (see below).

The KIE measured for direct reduction of GO by 1-*O*-methyl-6,6′-di-[^{2}H]-α-D-galactopyranoside reveals that the value measured in the steady-state represents a lower limit of isotope sensitivity of the catalytic reaction, and that the KIE is, in fact, much higher on the isolated substrate oxidation step, measured on k_{red} using transient kinetics methods (k_H/k_D = 21.1).[71] This observation is reinforced by evaluation of the substrate KIE using enzyme-monitored turnover measurements, which yields an estimate of k_H/k_D = 24.3, in good agreement with the value obtained for stoichiometric substrate oxidation. Enzyme-monitored turnover also suggest the existence of an additional, smaller, substrate KIE (k_H/k_D = 7.8) on the O_2 reoxidation step. This rather surprising result has been further investigated using oxygen uptake measurements, which demonstrate a striking substrate- and dioxygen-concentration dependence of the KIE on V/K (evaluated in the linear region of the reaction, [S] $\ll K_m$) [71] (Figure 12). The origin of this sensitivity can be traced to the ping pong kinetic mechanism underlying GO turnover. At low substrate concentrations, the overall turnover is rate-limited by substrate oxidation and the full substrate KIE is expressed. On the other hand, at high concentrations of the reducing substrate, reaction with O_2 becomes rate-limiting, and the observed KIE is reduced. The concentration of substrate at which the oxygen reaction becomes rate limiting depends on the oxygen concentration. Interestingly, the observed KIE does not approach a value of 1 at the highest substrate concentrations but, rather, a relatively large value near 8.5. This is close to the values previously reported for GO substrate oxidation obtained from extrapolation to infinite concentration of both substrates, suggesting that under those conditions, the overall rate is dominated by the

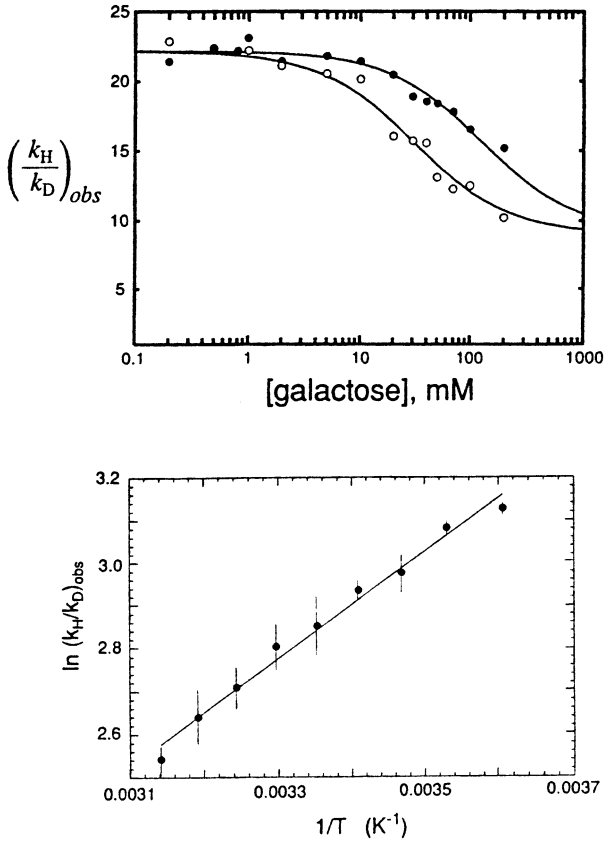

Figure 12. Oxygen and temperature dependence of galactose oxidase isotope effect from steady-state oxygen uptake. (top) Variation of the observed KIE on *V*/*K* with substrate concentration, for two dissolved oxygen concentrations, 360 mM (●) and 88 mM (○). (bottom) Temperature dependence of the observed KIE on *V*/*K*. (From ref 71.)

dioxygen reduction process. The substrate KIE also exhibits strong temperature dependence (Figure 12) implying a large activation parameter $E_a(D) - E_a(H) = 10.4$ kJ/mol, which exceeds the semiclassical upper limit of the effect of differences in zero-point energies on a barrier hopping trajectory. Extrapolating the temperature dependence of the KIE to infinite temperature yields an intercept value that is an estimate of the ratio of Arrhenius parameters for the protio and deuterio reactions, which for galactose oxidase substrate oxidation is found to be $A_H/A_D = 0.25$, below the absolute minimum lower limit based on semiclassical reaction theory. In combination, the anomalously high substrate oxidation KIE and anomalous values found for the temperature dependence of the KIE provide evidence for nonclassical behavior involved in substrate oxidation, including the possibility of hydrogen tunneling[94−96] during the reaction. Unusually large isotope effects have also been observed in quinoprotein amine dehydrogenases,[97,98] lipoxygenase,[99] and methane monooxygenase,[100] all of which are believed to have substrate oxidation mechanisms involving hydrogen atom tunneling. In the latter two examples, extremely large KIEs of 40−150 have been reported.[99,100]

A solvent isotope effect, attributed to the presence of a solvent molecule coordinated to the active site metal ion, has been reported for oxidation of 1-*O*-methyl-6,6′-di-[^{2}H]-α-D-galactopyranoside.[101] However, further investigation has shown that there is no detectable solvent KIE for this reaction ($k_H/k_D = 0.99 \pm 0.05$),[71] and that the earlier observation was likely an artifact resulting from partial inactivation of GO by contaminants in the deuterated solvent.

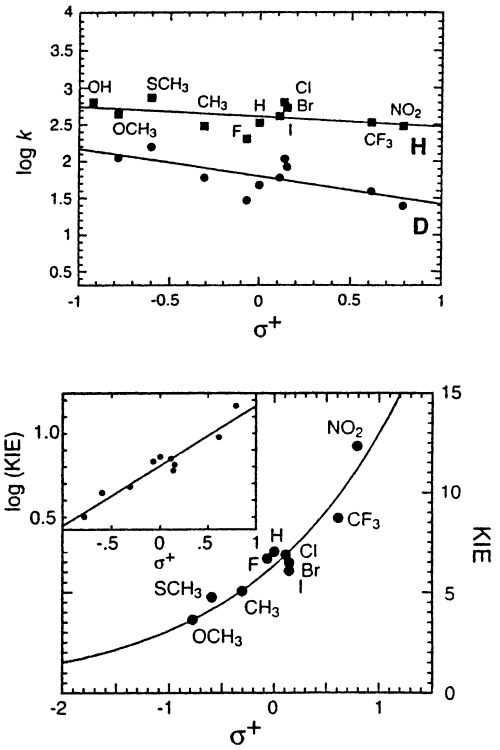

Figure 13. QSAR correlations for homologous benzyl alcohols. (top) Semilog linear free energy plot for para-substituted α,α′-protio (■) or α,α′-deuterio (●) benzyl alcohols over Hammett σ^+. Correlation slopes are shown ($\rho_H = -0.09 \pm 0.32$; $\rho_D = -0.49 \pm 0.61$). (bottom) Substituent dependence of the deuterium KIE on *V*/*K* for substrate oxidation. (From ref 102.)

C. Reaction Profile Analysis

Steady-state kinetics studies have been performed for a homologous series of benzyl alcohol derivatives with varying para substituents to explore the substituent effects on the substrate oxidation reaction.[102] Homologous benzyl alcohols have also proven useful in studies of flavoenzyme oxidases,[103] allowing the substrate to be systematically perturbed to probe the substrate oxidation mechanism. QSAR analysis[104,105] of the rate data for galactose oxidase over the entire substrate series indicates a very low level of correlation over the electronic substitutent parameter Hammett σ^+, corresponding to a reaction coefficient, $\rho = 0$ (Figure 13). The relative insensitivity of the substrate oxidation reaction to electronic effects ranging from strong electron withdrawal (−NO$_2$, −CF$_3$) to strong electron donation (−OH, −OCH$_3$) is remarkable. This type of weak dependence of the rate on the nature of the remote substituent is often cited as evidence for radical character (bond homolysis) or a cyclic transition state,[106] which avoids charge buildup or charge separation during the reaction.

Isotope effects on *V*/*K* from steady-state turnover measurements for this series of benzyl alcohols have also been subjected to QSAR analysis, revealing a

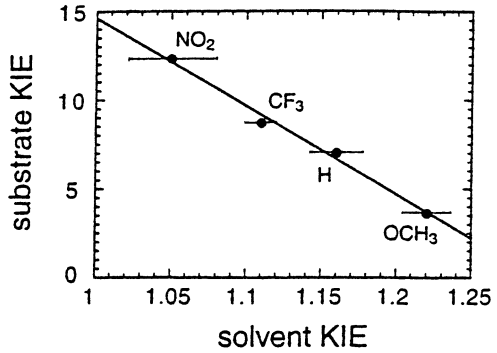

Figure 14. Anticorrelation of substrate and solvent kinetic isotope effects for galactose oxidase turnover with para-substituted benzyl alcohols. The horizontal and vertical bars indicate the magnitudes of the standard deviations. (From ref 102.)

strong log-linear correlation of the KIE with Hammett σ^+ (Figure 13). In contrast to the reaction rates themselves, the KIE values for the reactions exhibit a strong substituent dependence, ranging from 3.6 (for the *p*-methoxy derivative) to 12.3 (for the *p*-nitro compound). The sensitivity of the magnitude of the observed KIE for oxidation of α-deuterated benzyl alcohols to the nature of the substituent is somewhat surprising. Since KIEs reflect specific bond-making and bond-breaking contributions to the transition state of the reaction, smooth variation of KIE with the electronic component of the substituent perturbation must reflect a smooth change in the extent to which C−H bond cleavage dominates the transition state through this series of substrates. However, the relatively small rate dependence implies that the activation energy is fairly constant over this series. The correlation between KIE and the alcohol redox potential suggests an increase in C−H bond-breaking character for substrates that are more difficult to oxidize, possibly revealing a competition between electron transfer and atom transfer components of the reaction (see below).

A change in the nature of the transition state is also apparent in the values of the SKIE found for these reactions, which range from $k_{H2O}/k_{D2O} = 1.22 \pm .02$ (for 4-methoxybenzyl alcohol oxidation) to $k_{H2O}/k_{D2O} = 1.05 \pm 0.03$ for 4-nitrobenzyl alcohol (Figure 14). Fractionation factors for the ground state solvent isotope-exchange equilibria are expected to be very close to 1 for both reactant and product complexes, so the observed SKIE represents the full extent of the isotope effect associated with the exchangeable proton. In reactions for which PT is fully rate limiting, SKIEs in the range $k_{H2O}/k_{D2O} = 3-5$ have been reported. The smaller SKIE associated with benzyl alcohol oxidation suggests either that PT character does not dominate the transition state or that the hydrogen bond through which PT occurs is very weak. The former explanation suggests that a large SET contribution in the transition state accounts for the modest isotope-sensitivity of these reactions. The correlation of reactivity over a homologous set of substrates forms the basis for analysis of the profile of the substrate oxidation reaction (see below).

D. Mechanism-Based Inactivation by Substrate Analogues

The mechanism of galactose oxidase has also been probed using alcohol derivatives which stoichiometrically inactivate the enzyme by a one-electron reduction pathway[93,107−109]. Some, including quadricyclane methanol round trip radical probe,[107] β-halo ethanols,[93] and phenylcyclopropylmethanols,[107] are potentially capable of rearranging during reaction via a ketyl intermediate, but no information is available on product distributions generated during the inactivation process. Thiol analogues have also been investigated in the inactivation studies.[109] Highly efficient inactivation is observed with all of these analogues, and significant KIEs are observed on the inactivation rate. All appear to convert the enzyme to the one-electron reduced, catalytically inactive form, implying that they serve as one-electron reductants toward the active site, although some processes exhibit unexplained multiphase kinetics. Since the copper remains in the oxidized, Cu(II) state, these reactions have been interpreted as evidence for free radical chemistry during substrate oxidation.

VII. Substrate Oxidation Mechanism

The emerging view of the galactose oxidase catalytic mechanism is a synthesis of the work described in the previous section and represents a minimalist picture of a reaction for which no resolved intermediates have yet been identified, involving proton transfer, single electron transfer, and hydrogen atom transfer components (Figure 15). The absence of detectable intermediates may itself be significant, reflecting the extremely simple character of the overall reaction, involving transfer of the elements of dihydrogen between sites, as illustrated in Figure 16.

A. Substrate Binding

Evidence for the structure of the galactose oxidase substrate complexes is indirect, since it has not yet proven possible to prepare crystals with substrate bound in the active site.[23] Crystals of GO soaked with substrate show a single specific interaction site in the N-terminal domain,[28] which likely represents a targeting feature of the enzyme structure, immobilizing the extracellular enzyme on polymeric carbohydrates. The difficulty of preparing a substrate complex for crystallography can be traced to the low affinity of substrate interactions ($K_d = 180$ mM estimated from rapid kinetics studies[71]). In addition, there may be complications associated with crystal packing of molecules in the lattice, interfering with access to the active site in the crystalline enzyme.

The evidence for direct coordination of substrate alcohols includes, first of all, the crystal structure of the active site revealing exchangeable solvent bound at the surface-exposed metal complex. Water, HOH, may be viewed as the simplest homologue of the alcohol series, ROH, and its complex interpreted as a substrate analogue complex. Other small molecules

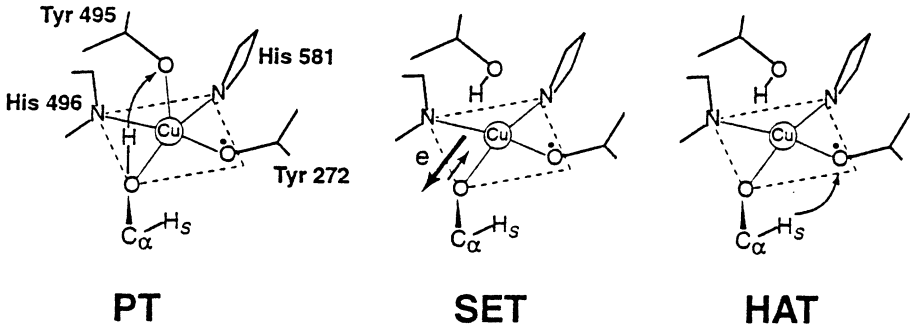

Figure 15. Elementary resolved components of the galactose oxidase substrate oxidation reaction. PT, proton transfer; SET, single electron transfer; HAT, hydrogen atom transfer. (From ref 102.)

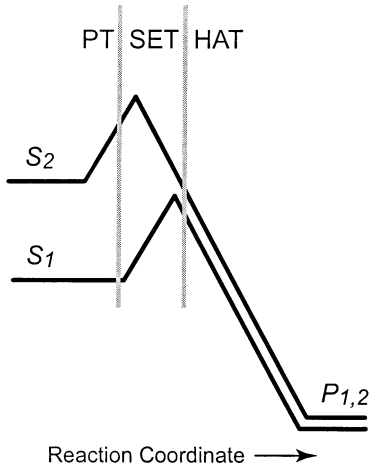

Figure 16. Turnover cycle proposed for galactose oxidase catalysis. (From ref 71.)

also have access to the active site, including acetate, which has been shown to directly coordinate to copper, replacing the exchangeable solvent in the complex. NMR relaxivity measurements also provide evidence that an alternative substrate for galactose oxidase (dihydroxyacetone) displaces the coordinated water in complexes with the catalytically inactive form of the enzyme.[110] In addition to the experimental evidence for substrate binding to copper, simple docking analysis as well as more elaborate molecular mechanics calculations provide theoretical justification for substrate binding in the active site and suggest a specific steric factor is responsible for the strong selectivity for galactose over glucose as substrate.[23,111] These studies also provide a rationale for the experimentally observed prochiral selectivity of hydrogen abstraction by galactose oxidase during turnover based on proximity of the *pro*-S hydrogen of the substrate to the Tyr272 oxygen in the most favorable binding mode.

B. Substrate Activation by Proton Abstraction

There is ample chemical precedence for activation of substrates for oxidation by deprotonation. Ionization of an alcohol has a dramatic effect on its redox potential, as well as the strength of the C−H bonds of the α-methylene group.[112] Direct coordination of alcohols to metal cations is known to significantly increase the acidity of the hydroxyl group through both electrostatic and covalent mechanisms. There is experimental evidence for a dramatic perturbation of the pK_a (>7 units) of simple alcohols bound to divalent metal ions.[113]

Ligand interactions with galactose oxidase also provide evidence for proton transfer processes in the active site. The proton uptake by Tyr495 associated with anion binding and the thermally driven solvent deprotonation in the active site complex reveals essential chemistry of the site.[49,53] Crystallographic data shows that the site undergoes a subtle reorganization between ligand-free and ligand-bound complexes that has been described in terms of a pseudorotation redefining the strong and weak interactions within the complex that may provide the driving force for proton abstraction. The observation of a significant solvent isotope effect on turnover of some substrates indicates that under some circumstances proton transfer may become partially rate-limiting for substrate oxidation. Proton abstraction may thus represent a gating process allowing the overall oxidation to proceed.

C. Electron Transfer and C–H Bond Cleavage

The chemistry of substrate oxidation involves loss of two electrons and cleavage of one of the C_α−H bonds within the hydroxymethylene headgroup of the substrate alcohol. The bond cleavage may in principle occur either through homolytic (hydrogen transfer) or heterolytic (hydride transfer) processes. Since there are two distinct sinks for the electrons in the metalloradical complex (Cu(II) metal ion and Tyr−Cys phenoxyl) the active site is clearly much better suited for a combination of SET and HAT processes. However, the ordering of these two processes is problematic.[71]

One-electron oxidation of the coordinated alkoxide anion by initial inner-sphere SET would reduce the metal center (Cu(II) → Cu(I)), forming an alkoxyl free radical (Scheme 4). The loss of one electron from the valence shell of the alcohol is predicted to strongly perturb the C−H bonding, providing a trigger for homolytic cleavage and hydrogen atom transfer reducing the Tyr−Cys phenoxyl. The sum of these two processes transforms the alcohol substrate into aldehyde product and leaves the enzyme in the fully reduced Cu(I) state. Alternatively, the ordering of the two processes may be reversed, with atom transfer (more generally, PCET) occurring initially, followed by inner sphere SET. In the latter case, the substrate is transformed sequentially through a ketyl radical (Scheme 4) which is capable of rapidly reducing the

Scheme 4. Free Radicals Generated by Alcohol Oxidation

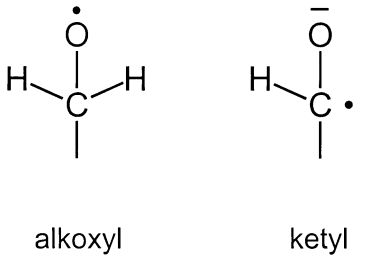

Scheme 5. Five-atom Cyclic Transition State for Substrate Oxidation by Galactose Oxidase

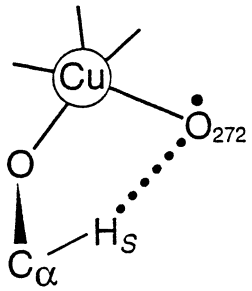

Cu(II). Both sequences result in the same overall transformation of the substrate and the active site.

The large substrate KIE that is observed in the reductive half-reaction clearly requires that the transition state for substrate oxidation includes substantial C−H bond cleavage character consistent with atom transfer. The presence of a phenoxyl acceptor in the active site argues in favor of hydrogen atom transfer rather than a more generalized sequential PCET process. The anomalously large values for the substrate KIE, even though they are well below the extreme values reported for some other enzymes, as well as the anomalous temperature dependence of the KIE, are both consistent with a tunneling contribution associated with atom transfer, which may occur through a five-atom ring transition state (Scheme 5). One of the important determinants for atomic tunneling is rigidity of the reactants,[75,76] and it is possible that the active site tryptophan (W290) contributes to the rigidity of the α-methylene in the complex.

The fact that the KIE is measured on a kinetic transient monitored as loss of absorption from the metalloradical complex suggests that atom transfer is the first event in substrate oxidation, since prior formation of a Cu(I) complex would mean that the complex expressing the isotope perturbation would lack the spectroscopic signal required for its detection. However, this assumes that discrete intermediates are formed along the reaction path. It appears more likely that substrate oxidation is a single-barrier process without resolved kinetic intermediates. The observation of smooth trends in the magnitude of the substrate KIE over a homologous series of alcohols[102] strongly supports a view in which substrate-level perturbations shift the transition state earlier or later along the reaction path thereby altering the kinetic sensitivity to different processes.

The effect of systematically varying the substrate properties has been interpreted in terms of mapping

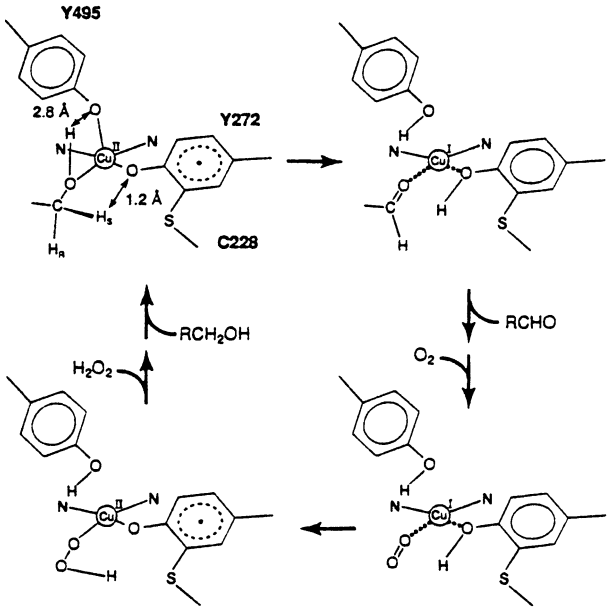

Figure 17. Reaction profile for substrate oxidation chemistry. Hypothetical reaction coordinates for two alternative substrates (S_1 and S_2) representing less easily oxidized (S_1) or more easily oxidized (S_2) variants are shown to illustrate the proposed correlation between the nature of the transition state and the overall driving force for the reaction.

a reaction profile for substrate oxidation. Substrates that are more difficult to oxidize (e.g., 4-nitrobenzyl alcohol) exhibit a large substrate KIE reflecting rate-limiting C−H bond cleavage, while the most easily oxidized substrates (e.g., 4-methoxybenzyl alcohol) exhibit a much smaller substrate KIE but a larger SKIE. The SKIE are expected to reflect the earliest contributions to the reaction associated with abstraction of the hydroxylic proton, implying that the rate-limiting contribution to the transition state is an isotope-insensitive SET process in that limit. It is important to distinguish between sequential processes associated with discrete activation barriers leading to the possibility of kinetic resolution of metastable intermediates, and the picture emerging from kinetic studies on galactose oxidase, pointing to a complex four-particle reaction coordinate without energetic resolution of individual steps (Figure 17). The fact that only the lightest species (electrons and protons) are required to move in this reaction distinguishes it from mechanisms involving molecular rearrangements that can give rise to intermediate-trapping barriers along the reaction coordinate.

The mechanistic significance of the antiferromagnetic coupling of free radical ligand and Cu(II) spins in the ground state of the metalloradical active site has yet to be determined[5,53,114]. Spin conservation in the substrate oxidation reaction provides a rationale for a diamagnetic active site, since both reactants and products are singlets, $S = 0$. This suggests the possibility that spin selection rules may apply to SET and HAT processes during substrate oxidation.[53]

VIII. Dioxygen Reduction

Much less is known about the mechanism of O_2 reduction, the second half-reaction comprising the

galactose oxidase turnover cycle. Although it is thought to represent the biologically relevant reaction, supplying hydrogen peroxide for extracellular peroxidases or as bacteriostatic agent, it is not required for galactose oxidase catalysis. Alternative oxidants, including hexacyanoferrate(III), can replace O_2 and support turnover under anaerobic conditions, although at a much lower rate than is found for the oxygen-driven reaction.[86]

The observation of a significant substrate KIE on the dioxygen reduction step is a particularly interesting aspect of the active site chemistry, in view of evidence that substrate oxidation and reaction with O_2 occur in distinct half reactions. If substrate oxidation is complete when dioxygen reduction occurs, there is no obvious reason for the latter reaction to be sensitive to substrate isotopic labeling. However, all the elements involved in O_2 reduction (two electrons and two protons) ultimately originate in the substrate molecule, and deuterium abstracted from the substrate alcohol during the oxidative half reaction may be retained in the active site between the two half reactions.[71] The KIE observed on O_2 reduction could then arise as a transferred isotope effect. The magnitude of the KIE for O_2 reduction (k_H/k_D = 8.5) would then imply that hydrogen transfer is fully rate limiting in the oxygen half-cycle.

One of the most important features of O_2 reduction chemistry in the GO active site is that it is nearly exclusively two-electron reaction. In other words, the amount of superoxide leaking from the active site during turnover (which results in a turnover-based inactivation of the enzyme) is small, and is estimated at <1 in 2000 turnovers.[86] Also, the active site does not appear to support further reduction of the initially formed peroxide product. The oxygenated complex is very unstable, so the structural basis for this controlled reactivity is still unclear, but the crystallographic data already available for the resting enzyme may provide a clue in the organization of solvent within the active site.[115] The stabilization of dioxygen species by proteins through hydrogen bonding interactions in some cases appears to be mimicked by water "ghosts" in the absence of dioxygen. A pair of water molecules resembling the dioxygen species reproduces some of the essential structural features of the oxygenated complex. In galactose oxidase, the active site contains a pair of solvent molecules, one coordinated to the copper ion and the other hydrogen bonded to the active site tyrosines. In the absence of other structural information, this suggests a model for a coordinated hydroperoxide product complex, which during turnover would subsequently be displaced by protonation of the coordinated oxygen atom.

IX. Conclusions

While much work remains to definitively resolve the outstanding questions of cofactor biogenesis and oxygen interactions, our understanding of the underlying chemistry of free radical catalysis by galactose oxidase has greatly increased in recent years. The combined structural, spectroscopic, and biochemical work has advanced the mechanistic insights into this remarkable metalloradical active site. Galactose oxidase is emerging as one of the best-characterized of the free radical enzymes, and the fundamental principles of free radical catalysis that are being revealed in detailed studies on galactose oxidase and other radical-copper oxidases may be expected to contribute to a better understanding of free radical mechanisms in other enzymes.

X. Abbreviations

EPR	electron paramagnetic resonance
ENDOR	electron nuclear double resonance
NMRD	nuclear magnetic relaxation dispersion
XANES	X-ray absorption near-edge structure
EXAFS	extended X-ray absorption fine structure
GO	galactose oxidase
AGO	oxidatively activated galactose oxidase
IAGO	eductively inactivated galactose oxidase
RGO	fully reduced, active galactose oxidase
SET	single electron transfer
HAT	hydrogen atom transfer
PCET	proton coupled electron transfer
PT	proton transfer
KIE	kinetic isotope effect
SKIE	solvent kinetic isotope effect
LLCT	ligand-to-ligand charge transfer
SOMO	spin-occupied molecular orbital

XI. Acknowledgment

Support for this work from the National Institutes of Health (GM46749) is gratefully acknowledged.

XII. References

(1) Whittaker, J. W. In *Advances in Protein Chemistry*; Richard, A., Gralla, E. B., Eds.; Academic Press: New York, 2002; Vol. 60.
(2) Hamilton, G. A. In *Copper Proteins*; Spiro, T. G., Ed.; Wiley: New York, 1981; pp 193−218.
(3) Ettinger, M. J.; Kosman, D. J. In *Copper Proteins*; Spiro, T. G., Ed.; Wiley: New York, 1981, pp 219−261.
(4) Whittaker, J. W. In *Metal Ions in Biological Systems*; Sigel, H., Ed.; Marcel Dekker: New York, 1994; Vol. 30, pp 315−360.
(5) Whittaker, J. W.; Whittaker, M. M. *Pure Appl. Chem.* **1998**, *70*, 903−910.
(6) Avigad, G.; Amaral, D.; Asensio, C.; Horecker, B. L. *J. Biol. Chem.* **1962**, *237*, 2736−2743.
(7) Whittaker, M. M.; Whittaker, J. W. *J. Biol. Chem.* **1988**, *263*, 6074−6080.
(8) Stubbe, J.; van der Donk, W. A. *Chem. Rev.* **1998**, *98*, 705−762.
(9) Frey, P. A. *Curr. Opin. Chem. Biol.* **1997**, *1*, 347−356.
(10) Marsh, E. N. *Bioessays* **1995**, *17*, 431−41.
(11) Pedersen, J. Z.; Finazzi-Agro, A. *FEBS Lett.* **1993**, *325*, 53−58.
(12) Brush, E. J.; Kozarich, J. W. In *Enzymes*; Sigman, D. S., Ed.; Academic Press: San Diego, 1992; Volume 20, pp 317−403.
(13) Frey, P. A. *Chem. Rev.* **1990**, *90*, 1343−1357.
(14) Stubbe, J. *Annu. Rev. Biochem.* **1989**, *58*, 257−285.
(15) Stubbe, J. *Biochemistry* **1988**, *27*, 3893−3900.
(16) Kersten, P. J.; Kirk, T. K. *J. Bacteriol.* **1987**, *169*, 2195−2201.
(17) Kersten, P. J. *Proc. Natl. Acad. Sci. U.S.A.* **1990**, *87*, 2936−2940.
(18) Kersten, P. J.; Cullen, D. *Proc. Natl. Acad. Sci. U.S.A.* **1993**, *90*, 7411−7413.
(19) Whittaker, M. M.; Kersten, P. J, Nakamura, N.; Sanders-Loehr, J.; Schweizer, E. S.; Whittaker, J. W. *J. Biol. Chem.* **1996**, *271*, 681−687.
(20) Hammel, K. E.; Mozuch, M. D.; Jensen, K. A., Jr.; Kersten, P. J. *Biochemistry* **1994**, *33*, 13349−13354.
(21) Silakowski, B. Ehret, H.; Schairer, U. *J. Bacteriol.* **1998**, *180*, 1241−1247.
(22) Dworkin, M. *Microbiol. Rev.* **1996**, *60*, 70−102.
(23) Knowles, P. F.; Ito, N. *Perspect. Bioinorg. Chem.* **1993**, *2*, 207−244.
(24) Jazdzewski, B. A.; Tolman, W. B. *Coord. Chem. Rev.* **2000**, *200−202*, 633−685.
(25) Itoh, S.; Taki, M.; Fukuzumi, S. *Coord. Chem Rev.* **2000**, *198*, 3−20.
(26) Siegbahn, P. E. M. *Chem. Rev.* **2003**, *103*, 2421−2456.

(27) Klinman, J. P. *Chem. Rev.* **1996**, *96*, 2541−2561.
(28) Ito, N.; Phillips, S. E. V.; Yadav, K. D. S.; and Knowles, P. F. *J. Mol. Biol.* **1994**, *238*, 794−814.
(29) Ito, N.; Phillips, S. E. V.; Stevens, C.; Ogel, Z.; McPherson, M. J.; Keen, J. N.; Yadav, K. P. D. S.; Knowles, P. F. *Faraday Discuss.* **1992**, *93*, 75−84.
(30) McPherson, M. J.; Parsons, M. R.; Spooner, R. K.; Wilmot, C. R. In *Handbook of Metalloproteins*; Messerschmidt, A.; Huber, R., Wieghardt, K., Poulos, T., Eds.; Wiley: Hoboken, NJ2001; pp 1272−1283.
(31) Sayle, R.; Milner-White, E. J. *Trends Biochem. Sci.* **1995**, *20*, 374.
(32) Bork, P.; Doolittle, R. F. *J. Mol. Biol.* **1994**, *236*, 1277−1282.
(33) Buschiazzo, A.; Tavares, G. A.; Campetella, O.; Spinelli, S.; Cremona, M. L.; París, G.; Fernanda Amaya, M.; Frasch, A. C. C.; Alzari, P. M. *EMBO J.* **2000**, *19*, 16−24.
(34) Chen, L.; Doi, M.; Durley, R. C. E.; Chistoserdov, A. Y.; Lidstrom, M. E.; Davidson, V. L.; Mathews, F. S. *J. Mol. Biol.* **1998**, *276*, 131−149.
(35) Xia, Z.-X.; He, Y.-N.; Dai, W.-W.; White, S. A.; Boyd, G. D.; Mathews, F. S. *Biochemistry* **1999**, *38*, 1214−1220.
(36) Brown, K.; Roig-Zamboni, V.; Cutruzzola, F.; Arese, M.; Sun, W.; Brunori, M.; Cambillau, C.; Tegoni, M. *J. Mol. Biol.* **2001**, *312*, 541−554.
(37) Farrugia, L. J. *J. Appl. Crystallogr.* **1997**, *30*, 565.
(38) Whittaker, J. W.; Whittaker, M. M. *Pure Appl. Chem.* **1998**, *70*, 903−910.
(39) Clark, K.; Penner-Hahn, J. E.; Whittaker, M. M.; Whittaker, J. W. *J. Am. Chem. Soc.* **1990**, *112*, 6433−6434.
(40) Clark, K.; Penner-Hahn, J. E.; Whittaker, M.; Whittaker, J. W. *Biochemistry* **1994**, *33*, 12553−12557.
(41) Ito, N.; Phillips, S. E. V.; Stevens, C.; Ogel, Z. B.; McPherson, M. J.; Keen, J. N.; Yadav, K. D. S.; Knowles, P. F. *Nature* **1991**, *350*, 87−90.
(42) Rogers, M. S.; Baron, A. J.; McPherson, M. J.; Knowles, P. F.; Dooley, D. M. *J. Am. Chem. Soc.* **2000**, *122*, 990−991.
(43) Whittaker, M. M.; Whittaker, J. W. *J. Biol. Chem.* **1990**, *265*, 9610−9613.
(44) Babcock, G. T.; El-Deeb, M. K.; Sandusky, P. O.; Whittaker, M. M.; Whittaker, J. W. *J. Am. Chem. Soc.* **1992**, *114*, 3727−3734.
(45) Gerfen, G. A.; Bellew, B.; Griffin, R.; Singel, D.; Ekberg, C. A.; Whittaker, J. W. *J. Phys. Chem.* **1996**, *100*, 16739−16748.
(46) Baron, A. J.; Stevens, C.; Wilmot, C.; Seneviratne, K. D.; Blakely, V.; Dooley, D. M.; Phillips, S. E. V.; Knowles, P. F.; McPherson, M. J. *J. Biol. Chem.* **1994**, *269*, 25095−25105.
(47) McPherson, M. J.; Stevens, C.; Baron, A. J.; Ogel, Z. B.; Senevriatne, K.; Wilmot, C.; Ito, N.; Brocklebank, I.; Phillips, S. E. V.; Knowles, P. F. *Biochem. Soc. Trans.* **1993**, *21*, 752−756.
(48) Whittaker, M. M.; Kersten, P. J.; Cullen, D.; Whittaker, J. W. *J. Biol. Chem.* **1999**, *274*, 36226−36232.
(49) Whittaker, M. M.; Whittaker, J. W. *Biophys. J.* **1993**, *64*, 762−772.
(50) Reynolds, M. P.; Baron, A. J.; Wilmot, C.; Phillips, S. E. V.; Knowles, P. F.; McPherson, M. J. *Biochem. Soc. Trans.* **1995**, *23*, 510S.
(51) Reynolds, M. P.; Baron, A. J.; Wilmot, C. M.; Vinecombe, E.; Stevens, C.; Phillips, S. E. V.; Knowles, P. F.; McPherson, M. J. *J. Biol. Inorg. Chem.* **1997**, *2*, 327−335.
(52) Rogers, M. S.; Knowles, P. F.; Baron, A. J.; McPherson, M. J.; Dooley, D. M. *Inorg. Chim. Acta* **1998**, *275−276*, 175−181.
(53) Whittaker, M. M.; Ekberg, C. A.; Peterson, J.; Sendova, M. S.; Day, E. P.; Whittaker, J. W. *J. Mol. Catal. B* **2000**, *8*, 3−15.
(54) Saysell, C. G.; Barna, T.; Borman, C. D.; Baron, A. J.; McPherson, M. J.; Sykes, A. G. *J. Biol. Inorg. Chem.* **1997**, *2*, 702−709.
(55) Bennati, M.; Farrar, C. T.; Bryant, J. A.; Inati, S. J.; Weiss, V.; Gerfen, G. J.; Riggs-Gelasco, P.; Stubbe, J.; Griffin, R. G. *J. Magn. Res.* **1999**, *138*, 232−243.
(56) Whittaker, M. M.; Chuang, Y. Y.; Whittaker, J. W. *J. Am. Chem. Soc.* **1993**, *115*, 10029−10035.
(57) Itoh, S.; Takayama, S.; Arakawa, R.; Furuta, A.; Komatsu, M.; Ishida, A.; Takamuku, S.; Fukuzumi, S. *Inorg. Chem.* **1997**, *36*, 1407−1416.
(58) Itoh, S.; Hirano, K.; Furuta, A.; Komatsu, M.; Ohshiro, Y.; Ishida, A.; Takamuku, S.; Kohzuma, T.; Nakamura, N.; Suzuki, S. *Chem. Lett. (Jpn.)* **1993**, 2099−2102.
(59) Himo, F.; Eriksson, L. A.; Blomberg, M. R. A.; Siegbahn, P. E. M. *Int. J. Quantum Chem.* **2000**, *76*, 714−723.
(60) Himo, F.; Babcock, G. T.; Eriksson, L. A. *Chem. Phys. Lett.* **1999**, *313*, 374−378.
(61) Engström, M.; Himo, F.; Ågren, H. *Chem. Phys. Lett.* **2000**, *319*, 191−196.
(62) Wise, K. E.; Pate, J. B.; Wheeler, R. A. *J. Phys. Chem. B* **1999**, *103*, 4764−4772.
(63) Schaftenaar, G. *J. Comput.-Aided Mol. Des.* **2001**, *14*, 123−134.
(64) Whittaker, M. M.; Whittaker, J. W. *Protein Exp. Purif.* **2000**, *20*, 105−111.
(65) Day, E. P. *Methods Enzymol.* **1993**, *227*, 437−463.
(66) McGlashin, M. L.; Eads, D. D.; Spiro, T. G.; Whittaker, J. W. *J. Phys. Chem.* **1995**, *99*, 4918−4922.
(67) Wright, C. R.; Sykes, A. G. *J. Inorg. Biochem.* **2001**, *85*, 237−243.
(68) Wachter, R.; Branchaud, B. P. *Biochim. Biophys. Acta* **1998**, *1384*, 43−54.
(69) Wright, C. R.; Sykes, A. G. *Inorg. Chem.* **2001**, *40*, 2528−2533.
(70) Borman, C. D.; Wright, C.; Twitchett, M. B.; Salmon, G. A.; Sykes, A. G. *Inorg. Chem.* **2002**, *41*, 2158−2163.
(71) Whittaker, M. M.; Ballou, D. P.; and Whittaker, J. W. *Biochemistry* **1998**, *37*, 8426−8436.
(72) Gray, H. B.; Winkler, J. R. *Annu. Rev. Biochem.* **1996**, *65*, 537−61.
(73) Onuchic, J. N.; Beratan, J. N.; Winkler, J. R.; Gray, H. B. *Annu. Rev. Biophys. Biomol. Struct.* **1992**, *21*, 349−77.
(74) Cha, Y.; Murray, C. J.; Klinman, J. P. *Science* **1989**, *243*, 1325−1330.
(75) Klinman, J. P. *Trends Biochem. Sci.* **1989**, *14*, 368−373.
(76) Kohen, A.; Klinman, J. P. *Chem. Biol.* **1999**, *6*, R191−R198.
(77) Bahnson, B. J.; Colby, T. D.; Chin, J. K.; Goldstein, B. M.; Klinman, J. P. *Proc. Natl. Acad. Sci. U.S.A.* **1997**, *94*, 12797−127802.
(78) Bahnson, B. J.; Klinman, J. P. *Methods Enzymol.* **1995**, *249*, 373−397.
(79) Mayer, J. M. *Acc. Chem. Res.* **1998**, *31*, 441−450.
(80) Lucarini, M.; Pedrielli, P.; Pedulli, G. F. *J. Org. Chem.* **1996**, *61*, 9259−9263.
(81) Foti, M.; Ingold, K. U.; Lusztyk, J. *J. Am. Chem. Soc.* **1994**, *116*, 9440−9447.
(82) Cukier, R. I. *J. Phys. Chem.* **1994**, *98*, 2377−2381.
(83) Fang, J.-Y.; Hammes-Schiffer, S. *J. Chem. Phys.* **1997**, *106*, 8442−8454.
(84) Kwiatkowski, L. D.; Adelman, M.; Pennelly, R.; Kosman, D. J. *J. Inorg. Biochem.* **1981**, *14*, 209−222.
(85) Kosman, D. J.; Ettinger, M. J.; Weiner, R. E.; Massaro, E. J. *Arch. Biochem. Biophys.* **1974**, *165*, 456−467.
(86) Hamilton, G. A.; Adolf, P. K.; de Jersey, J.; DuBois, G. C.; Dyrkacz, G. R.; Libby, R. D. *J. Am. Chem. Soc.* **1978**, *100*, 1899−1912.
(87) Tressel, P. S.; Kosman, D. J. *Methods Enzymol.* **1982**, *89*, 172−176.
(88) Patil, P. V.; Ballou, D. P. *Anal. Biochem.* **2000**, *286*, 187−192.
(89) Gibson, Q. H.; Swaboda, B. E. P.; Massey, V. *J. Biol. Chem.* **1964**, *250*, 4048−4052.
(90) Borman, C. D.; Saysell, C. G.; Sykes, A. G. *J. Biol. Inorg. Chem.* **1997**, *2*, 480−487.
(91) Maradufu, A.; Cree, G. M.; Perlin, A. S. *Can. J. Chem.* **1971**, *49*, 3429−3437.
(92) Villafranca, J. J.; Freeman, J. C.; Kotchevar, A. In *Bioinorganic Chemistry of Copper*; Karlin, K. D., Tyeklar, Z., Eds.; Chapman and Hall: New York, 1993; pp 439−446.
(93) Wachter, R. M.; Montague-Smith, M. P.; Branchaud, B. P. *J. Am. Chem. Soc.* **1997**, *119*, 7743−7749.
(94) Melander, L.; Saunders, W. H., Jr. *Reaction Rates of Isotopic Molecules*; Krieger Publishing Co.: Malabar, FL, 1987.
(95) Schneider, M. E.; Stern, H. J. *J. Am. Chem. Soc.* **1972**, *94*, 1517−1522.
(96) Bell, R. P. *The Tunnel Effect in Chemistry*; Chapman and Hall: New York, 1980.
(97) Hyun, Y. L.; Zhu, Z.; Davidson, V. L. *J. Biol. Chem.* **1999**, *274*, 29081−29086.
(98) Brooks, H. B.; Jones, L. H.; Davidson, V. L. *Biochemistry* **1993**, *32*, 2725−2729.
(99) Rickert, K. W.; Klinman, J. P. *Biochemistry* **1999**, *38*, 12218−12228.
(100) Nesheim, J. C.; Lipscomb, J. D. *Biochemistry* **1996**, *35*, 10240−10247.
(101) Driscoll, J. J.; Kosman, D. J. *Biochemistry* **1987**, *26*, 3429−3436.
(102) Whittaker, M. M.; Whittaker, J. W. *Biochemistry* **2001**, *40*, 7140−7148.
(103) Menon, V.; Hsieh, C.-T.; Fitzpatrick, P. F. *Bioorganic Chem.* **1995**, *23*, 42−53.
(104) Hansch, C.; Leo, A. *Exploring QSAR. Fundamentals and Applications in Chemistry and Biology*; American Chemical Society: Washington, DC, 1995.
(105) Hansch, C.; Leo, A. *Exploring QSAR. Hydrophobic, Electronic, and Steric Constants*; American Chemical Society: Washington, DC, 1995.
(106) Gilliom, R. D. In *Introduction to Physical Organic Chemistry*; Addison-Wesley: New York, 1970; p 214.
(107) Branchaud, B. P.; Montague-Smith, M. P.; Kosman, D. J.; McLaren, F. R. *J. Am. Chem. Soc.* **1993**, *115*, 798−800.
(108) Turner, B. E.; Branchaud, B. P. *Bioorg. Med. Chem. Lett.* **1999**, *9*, 3341−3346.
(109) Wachter, R.; Branchaud, B. P. *Biochemistry* **1996**, *35*, 14425−14435.
(110) Knowles, P. F.; Brown, R. D., III.; Koenig, S. H.; Wang, S.; Scott, R. A.; McGuirl, M. A.; Brown, D. E.; Dooley, D. M. *Inorg. Chem.* **1995**, *34*, 3895−3902.

(111) Wachter, R.; Branchaud, B. P. *J. Am. Chem. Soc.* **1996**, *118*, 2782−2787.
(112) Steigerwald, M. L.; Goddard, W. A., III.; Evans, D. A. *J. Am. Chem. Soc.* **1979**, *101*, 1994−1997.
(113) Kimura, E.; Nakamura, I.; Koike, T.; Shionoya, M.; Kodama, Y.; Ikeda, T.; Shiro, M. *J. Am. Chem. Soc.* **1994**, *116*, 4764−4771.
(114) Müller, J.; Weyhermüller, T.; Bill, E.; Hildebrandt, P.; Ould-Moussa, L.; Glaser, T.; Wieghardt, K. *Angew. Chem., Int. Ed. Engl.* **1998**, *37*, 616−619.
(115) Whittaker, J. W. *Essays Biochem.* **1999**, *34*, 155−172.

CR020425Z